Chapter 5

Maps of CG 22

5.1 Introduction

In this chapter we derive the mass of Blob 1 of CG22. This globule has three regions of high obscuration along its tail which may, in fact, be seperate CGs. These have been called Blob 1,2 and 3 respectively. From the maps of the Blob 1 arid associated tail of CG 22 made in the J=1 → 0 lines of ^{12}CO and ^{13}CO we derive temperature and column density distributions. We estimate the mass of Blob 1 by three different methods. The chapter ends with a discussion of the results.

5.2 Data Reduction

The observations and basic data reduction have been described in chapter 3. The temperature scale obtained by these reduction steps is what has been called T_A^* in the literature. This quantity is telescope dependent. We have to correct this further for the forward coupling efficiency and the image-band to signal-band gain-ratio to obtain T_R^*, the main beam antenna temperature. This quantity has also been called the radiation temperature. This is the closest one can get to the source brightness temperature in the absence of any knowledge about the source structure, and is less dependent on the telescope. We describe below briefly the basis of these corrections.

5.3 Basics of calibration

An observation consists of a run of ON and OFF measurements, and a run of AMB and OFF measurements for calibration. The ON and OFF measurements may correspond to two different positions in the sky (beam or position switching) or two different frequencies (frequency switching) and the AMB measurement is made with an ambient temperature absorber in front of the receiver. Let the corresponding voltages measured he V_{ON}, V_{OFF} and V_{AMB}. Let the system, including the atmosphere, have gains G_s and G_i in the signal arid image bands. Then for a spectral line observation with a double side-band (DSB) system we have

$$V_{ON} = G_s T_{sys,s} + G_i T_{sys,i} + G_s T_{source} \quad (5.1)$$

$$V_{OFF} = G_s T_{sys,s} + G_i T_{sys,i} \quad (5.2)$$

$$V_{AMB} = G_s T_{sys,s} + G_i T_{sys,i} + (G_s + G_i) T_{amb} \quad (5.3)$$

from which we derive

$$T_{source} = T_{AMB}(1 + \frac{G_i}{G_s})\frac{V_{ON} - V_{OFF}}{V_{AMB} - V_{OFF}} \quad (5.4)$$

T_{source} is what is normally referred to as T_A^* in literature, the antenna temperature after correction for all telescope losses occuring at ambient temperature (for example, a lossy element at room temperature in the beam path or beam truncation due to or spill-over onto ambient temperature objects). It is not corrected for that part of the telescope response on the sky outside the main beam due to spill over past the secondary, the error pattern etc. This correction is done by dividing T_A^* by η_{fss}, the forward spill over and scattering efficiency.

5.4 Calibration at the 10.4m telescope

For the DSB receivers used at the 10.4m telescope, tlie ratio of tlie side-band gains have been measured to be same within 0.5dB. We assume that the gains are same because the signal and image frequencies are only 3 GHz apart. So G_s ane G; can be different only because of tlie frequency dependence of atmospheric absorption. The measured atmospheric absorption in the 3 mm window reproduced in figure 5.1 from Ulich and Haas(1976) shows that the frequency dependence is appreciable at 115 GHz arid needs to be taken into account. We estimate the ratio G_i/G_s from this figure to be $e^{0.17}$ for ^{12}CO observations with LO at 113.8 GHz. The measurements do not necessarily correspond to conditions at Bangalore but we assume that the effect on tlie gain ratio will only he of second order. So all our ^{12}CO line strengths liave to be multiplied by a factor $(1 + e^{0.17})/2 = 1.09$. As can be seen from the figure, the atmospheric absorption flattens off at 110 GHz and therefore ^{13}CO line strengths do not need such a correction. To make tlie more important correction for forward spill over and scattering, we can use the measured value of 0.61 for η_{fss} at 113.8 GHz (Patel, 1990). We assume that η_{fss} is 0.61 at both 110 GHz and 115 GHz and multiply both ^{12}CO and ^{13}CO data by $1/\eta_{fss} = 1.64$. By doing this we get what is referred to as T_R^*, the source *brightness temperature convolved* with the antenna *diffraction* pattern, tlie closest one can get to the source brightness temperature in the absence of any knowledge about the source structure. This is the quantity that is reported nowadays in tlie literature. So *the correction factors* to be applied *for* ^{12}CO and ^{13}CO *data* are 1.79 and *1.64, respectively.* On applying these corrections the line strengths on Orion **A** obtained at tlie 10.4m telescope are 73.4 K for ^{12}CO and 13.9 K for ^{13}CO in agreement with values reported in tlie literature. Table 5.1 lists the values obtained by various telescopes.

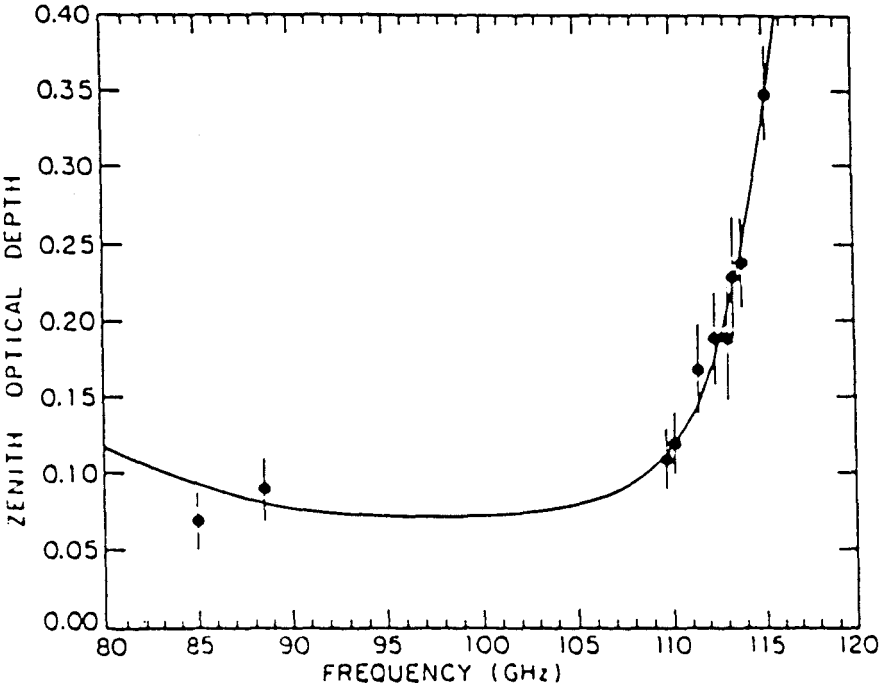

Figure 5.1: The atmospheric attenuation curve over the 3-mm window (after Ulich and Haas 1976).

Table 5.1: CO line strengths on ORI A				
Telescope	^{12}CO K	^{13}CO K	beam "	ref.
FCRAO 14m	70	17	50	Snell et. *al.* 1984.
AT&T Bell Labs 71n	76	14.9	100	Bally et. al. 1987.
RRI 10.4m	73.4	13.9	60	

The forward spill over and scattering efficiency, η_{fss}, is a function of elevation but since all the data for the maps were taken over a small elevation range of 25°-40°, we do not make any elevation dependent corrections. The T_R^* for Orion A values quoted above were made at ~45° elevation. We assume that the correction applied is not much in error for the elevation range of our observations.

The final spectra were written on tape in FITS format and further data reduction to obtain temperatures, optical depths arid column densities were carried out on AIPS. We give a brief summary of the methods used to derive these quantities and the results.

5.5 Temperature

The most common method used to determine the kinetic temperature in a molecular cloud is to use a line that is optically thick and thermalised. These conditions are met by the J=1 → 0 transition of ^{12}CO. Due to its small dipole moment, CO reaches thermal equilibrium for relatively low density of H_2 (300 cm^{-3}). In addition, this line is almost always optically thick. The disadvantage of this method is that tlie temperature obtained corresponds to the outer regions of the cloud where the line becomes optically thick. However, unless detailed modelling is done a constant temperature for the cloud is assumed even though this is unrealistic. Keeping in mind that for typical molecular cloud temperatures $h\nu \ll kT$ is not valid and taking into account the 2.7 K background. the kinetic temperature is given by

$$T_{kin} = \frac{5.532}{\ln(1 + \frac{5.532}{(T_{Lp}+0.8182)})} \tag{5.5}$$

as derived in the Appendix. Figures 5.2(a) arid (b) show a contour plot and a , psuedo-color image, respectively, of the distribution of T_{kin} in CG22-Blob 1.

5.6 Optical Depth

The spectral line from ^{12}CO being optically thick, it is ^{13}CO whose optical depth is determined directly from the observations. One first assumes that the excitation temperatures for both ^{12}CO and ^{13}CO are the same. Then one obtains the ^{13}CO optical depth from the observed ^{13}CO line using simple radiative transfer. We reproduce below the expression for optical depth derived in the Appendix:

$$\tau_{13} = -\ln\left[1 - \frac{T_{13}}{5.289}\left\{\left[e^{\frac{5.289}{T_{ex}}} - 1\right]^{-1} - 0.1642\right\}^{-1}\right] \tag{5.6}$$

Figures 5.3(a) and (b) show, respectively, a contour plot and a pseudo-color image of $\int \tau dv$, the integrated optical depth distribution in CG 22-Blob 1.

5.7 Column Density

To derive the column density $\mathcal{N}_{H_2}$ of molecular hydrogen, we first obtain the $\mathcal{N}_{^{13}CO}$, the column density of ^{13}CO from $\int \tau dv$ using the following relation derived in the Appendix:

$$\mathcal{N}_{^{13}CO} = 2.42 \times 10^{14} \frac{T_{ex} \int \tau_{13} dv}{(1 - e^{-5.289/T_{ex}})} \tag{5.7}$$

From $\mathcal{N}_{^{13}CO}$ we get $\mathcal{N}_{H_2}$ using the proportionality factor given by Dickman(1978) viz.,

$$\mathcal{N}_{H_2} = (5.0 \pm 2.5) \times 10^5 \mathcal{N}_{^{13}CO} \tag{5.8}$$

This conversion has been derived from observations of 38 'dark clouds in ^{12}CO and ^{13}CO and extinction measurements. A universal value for the ratio $\mathcal{N}_{H_2}/\mathcal{N}_{^{13}CO}$ has been questioned by Frerking, Langer and Wilson(1982) who found that this number can vary by as much as a factor of 10. We use Dickman's number as more information is not available. Figures 5.4(a) and (b) show a contour plot, and a pseudo-color image of the distribution of $\mathcal{N}_{^{13}CO}$ in CG 22-Blob 1.

5.8 Mass estimates

Masses for niolecular cloutls can be estimated by three different methods. The first method uses an optically thin line such as ^{13}CO to get $\mathcal{N}_{H_2}$ as done above. If tlie distance to tlie cloud is known, $\mathcal{N}_{H_2}$ can be integrated over tlie projected area of the

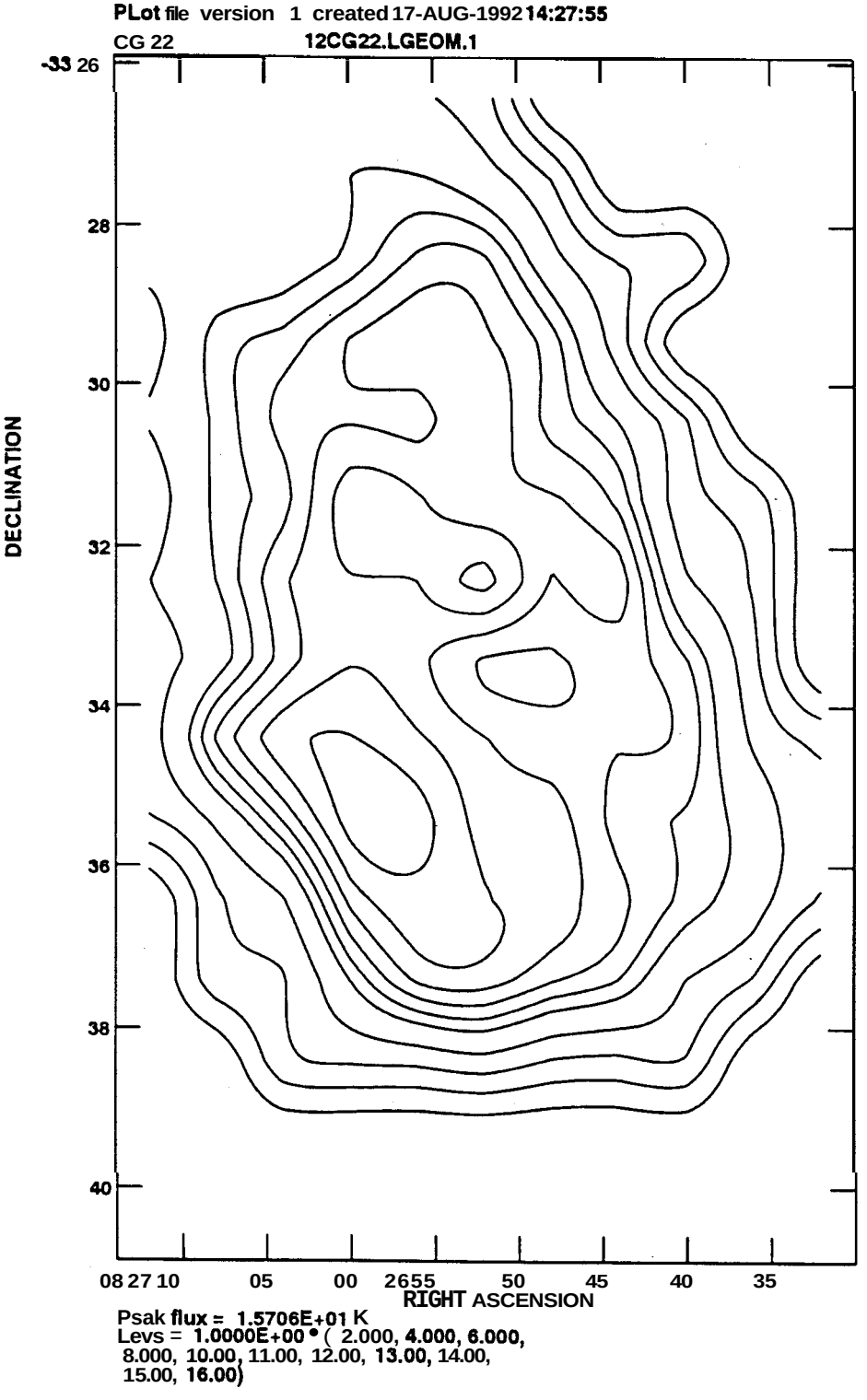

Figure 5.2 (a) A contour plot of the kinetic temperature distribution over CG22-Blob-1. The levels are in Kelvins. (From ^{12}CO observations)

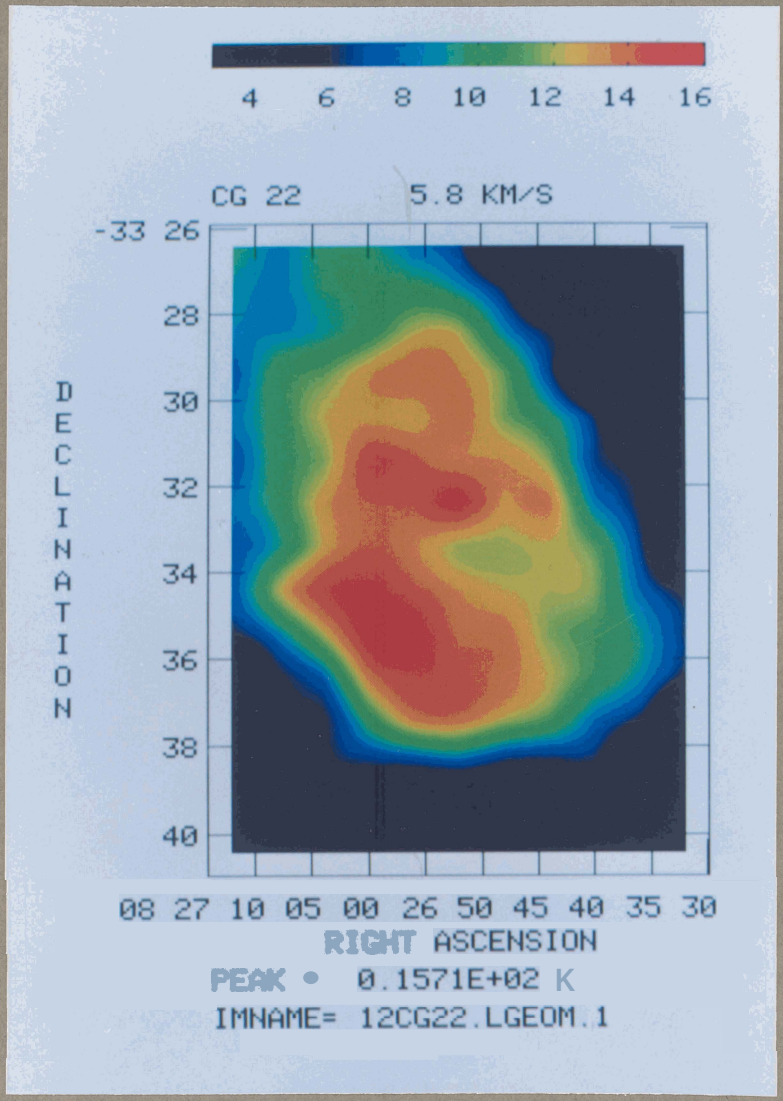

Figure 5.2 (b) **A pseudo color image of the kinetic temperature distribution** over CG22-Blob-1. **The scale is in units of Kelvin.**

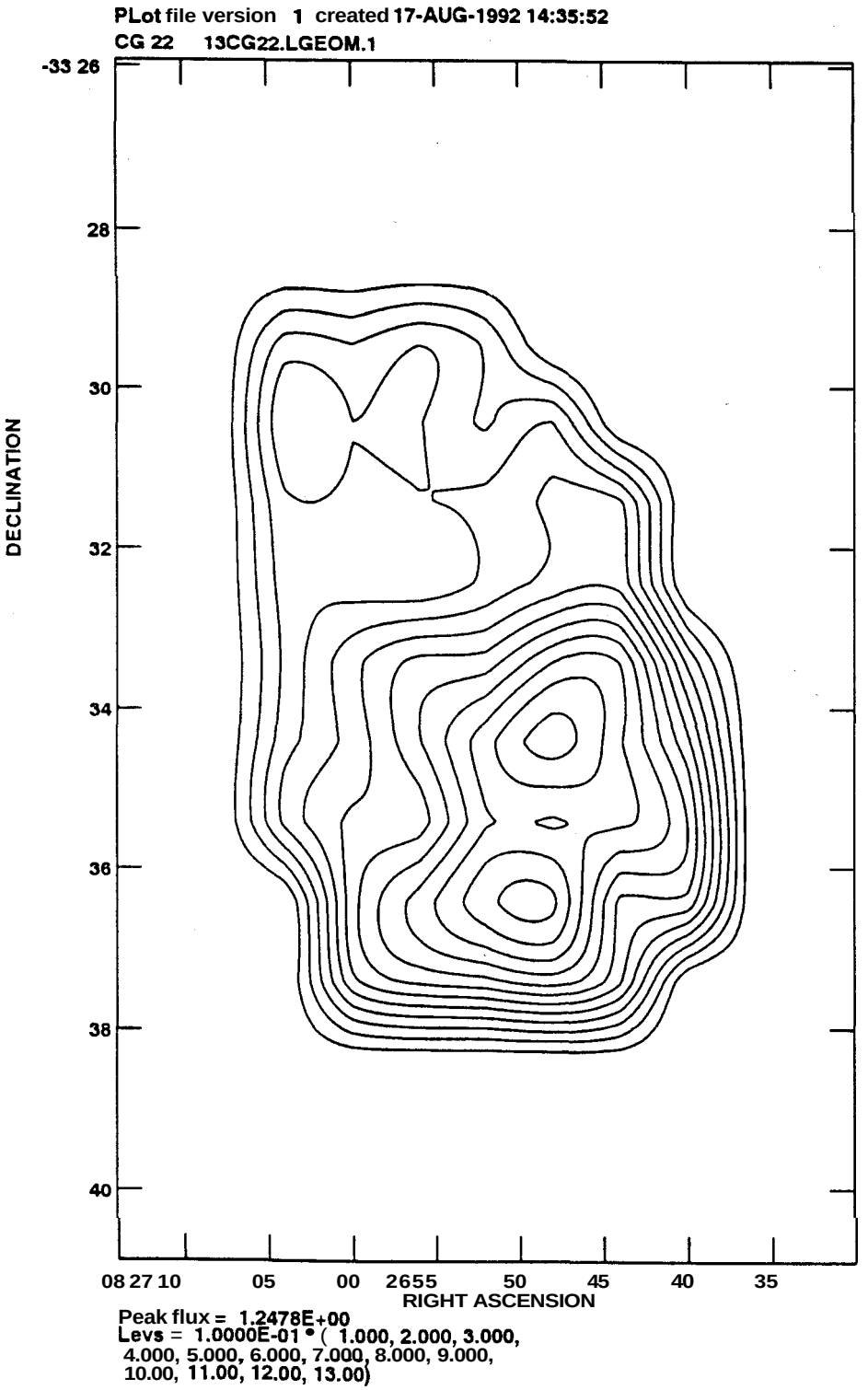

Figure 5.3 (a) A contour plot of the integrated ^{13}CO optical depth distribution over CG22-Blob-1.

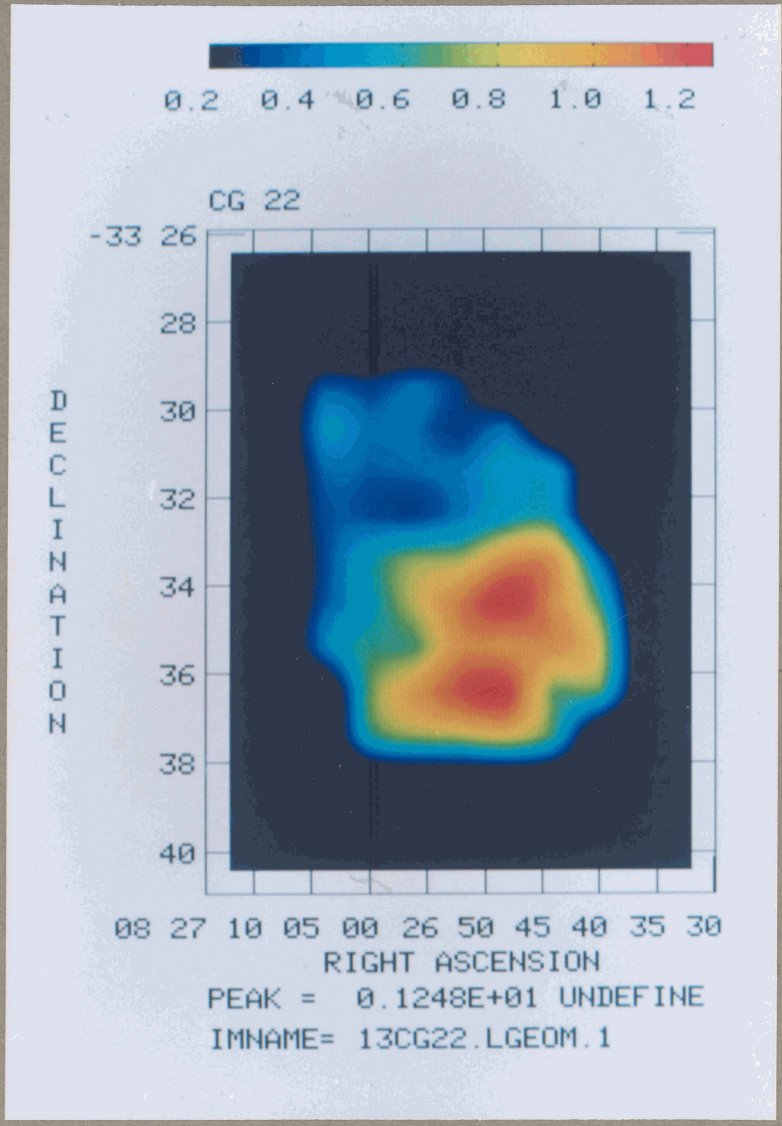

Figure **5.3** (b) A pseudo color image of the integrated ^{13}CO optical depth distribution over CG22-Blob-1.

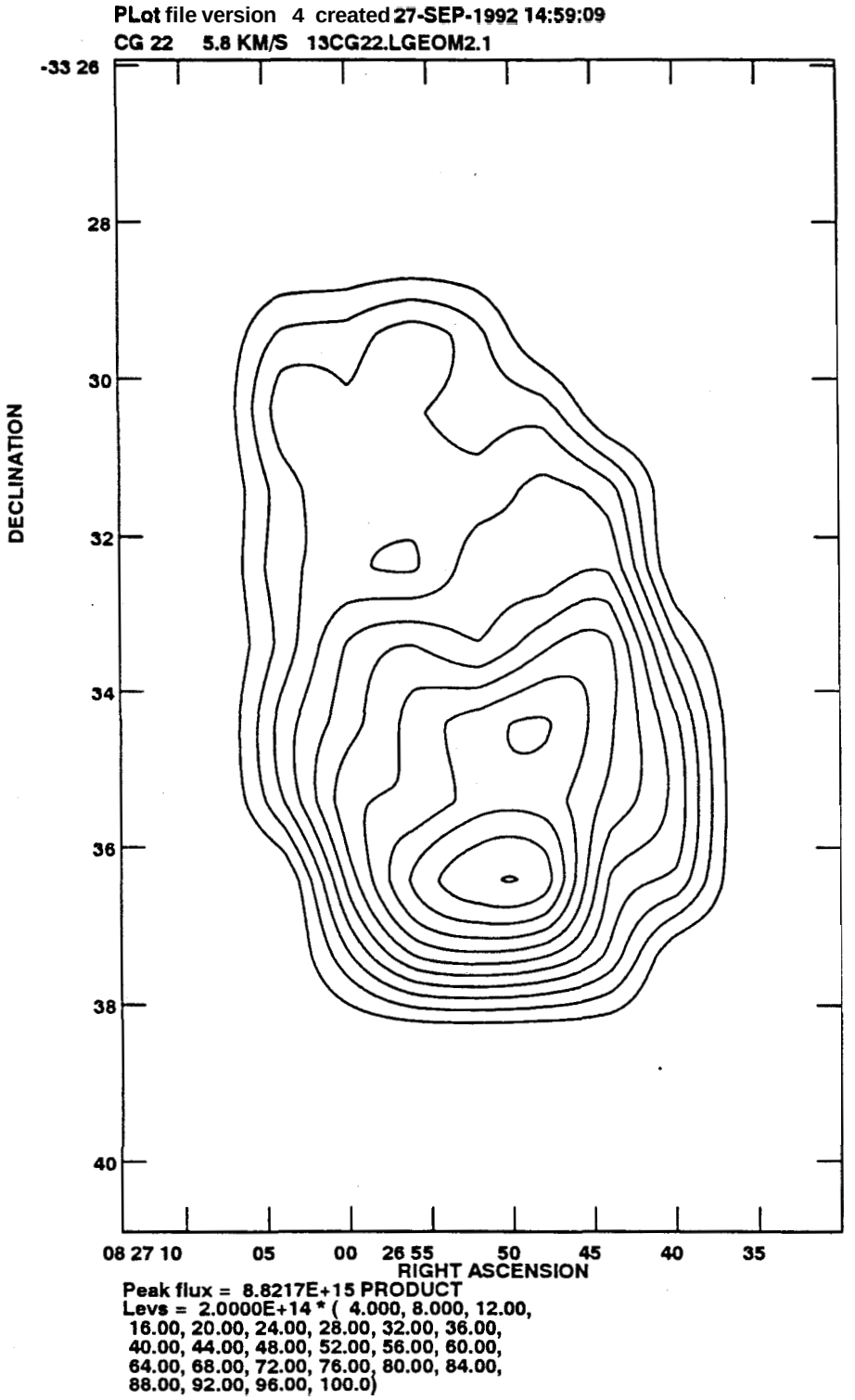

Figure 5.4 (a) A contour plot of the ^{13}CO column density distribution over CG22-Blob-1. The levels listed are in units of cm^{-2}.

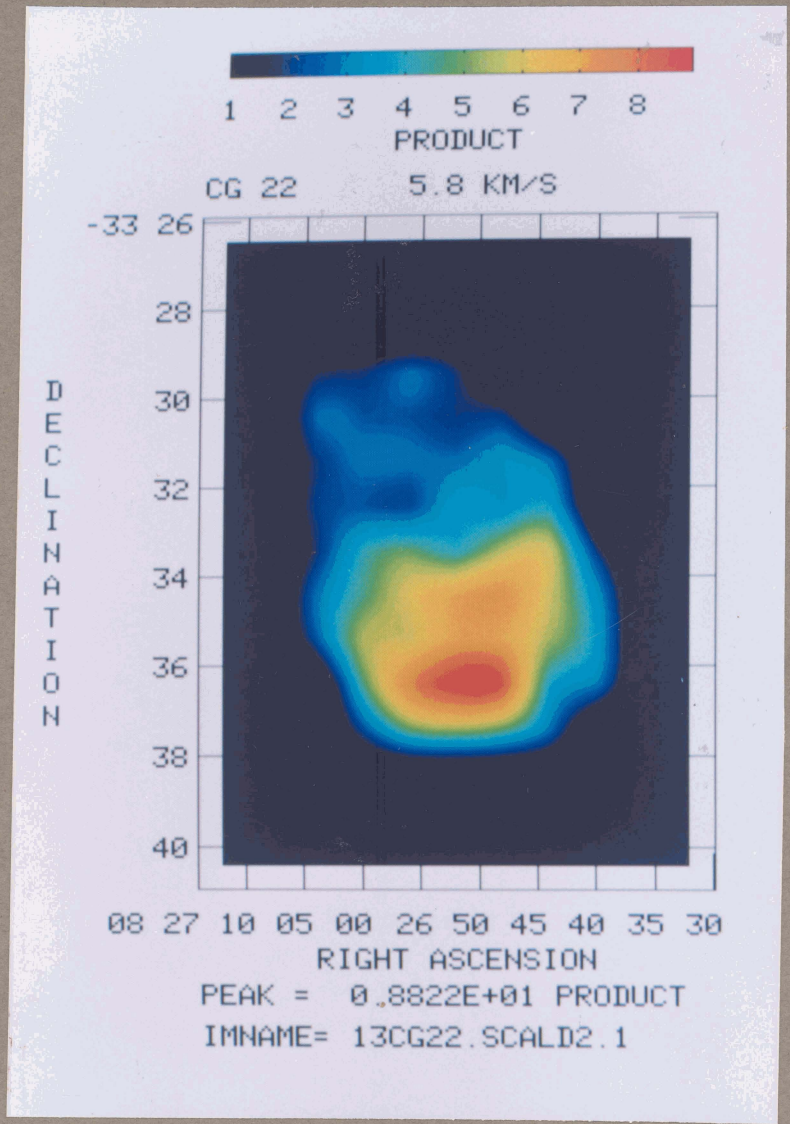

Figure 5.4 (b) A pseudo color image of the ^{13}CO column density distribution over CG22-Blob-1. The scale is in units of $10^{15} cm^{-2}$.

cloud to obtain the gas mass. Based on this method **we derive a mass of 27 $M_\odot$ for CG 22-Blob 1.**

The second method uses the empirically determined proportionality between $I_{^{12}CO}$ and $\mathcal{N}_{H_2}$ (Dickman 1978; Young and Scoville 1982). The basis for this proportionality has remained unclear although explanations based on the clumpy nature of molecular clouds and virial equilibrium have been proposed (Solomon *et. al.* 1987). We have used a value of 2.3×10^{20} $cm^{-2}/Kkms^{-1}$ for the ratio $I_{^{12}CO}/\mathcal{N}_{H2}$. **Based on this method we obtain a mass of 71$M_\odot$ for CG 22-Blob 1.**

The third method assumes that tlie cloud is in *virial equilibrium,* and estimates the mass from the observed velocity dispersion. Approximating CG 22-Blob 1 by a sphere with radius 5′, using the observed v_{FWHM} of 1.2 kms^{-1} **we obtain a virial mass of 250 $M_\odot$.**

5.9 Discussion

Figure 5.5 shows the ^{13}CO column density distribution superimposed on an optical picture of CG 22 from the ESO plates. Clearly, there is excellent agreement between the two. The individual streaks seen on tlie optical tail are well traced in CO. In addition, the CO emission is restricted to the regions delineated in the optical picture. The gradient in $\mathcal{N}_{^{13}CO}$ is quite sharp on tlie side which faces the center of the system of CGs (roughly south) whereas on the northern side the cloud is diffuse. These evidences point directly to the profound effect of tlie environment on the globule.

There is evidence for an embedded young star which shows up in the IRAS maps of Sahu *et.al.*(1989) as a point source. This star has been seen in 2.2μ scans and is the same as the Hα emission star Wra220 (also PHα92). This is believed to be a pre-main sequence star in the mass range 0.5-2 $M_\odot$ forming in CG 22- Blob 1. This makes the star formation efficiency of the globule $\sim$ *a few* percent. This point source has an IR luminosity of $\sim4L_\odot$ with a large error ($1L_\odot$-$8L_\odot$). The ratio L_{IR}/M is only 0.15. Sugitani *et.al.*(1989) have established an empirical criterion for externally triggered star formation based on this ratio. According to them a ratio $>$ 0.3 implies external mechanisms. It would appear that this star in CG 22 is not being formed by external mechanisms but it is not possible to say this conclusively because the error in L_{IR} is too large.

The mass derived here from CO observations (27-70$M_\odot$) is in reasonable agreement with the estimate ($\sim40M_\odot$) obtained by Sahu *et.al.*(1989) from tlie IRAS

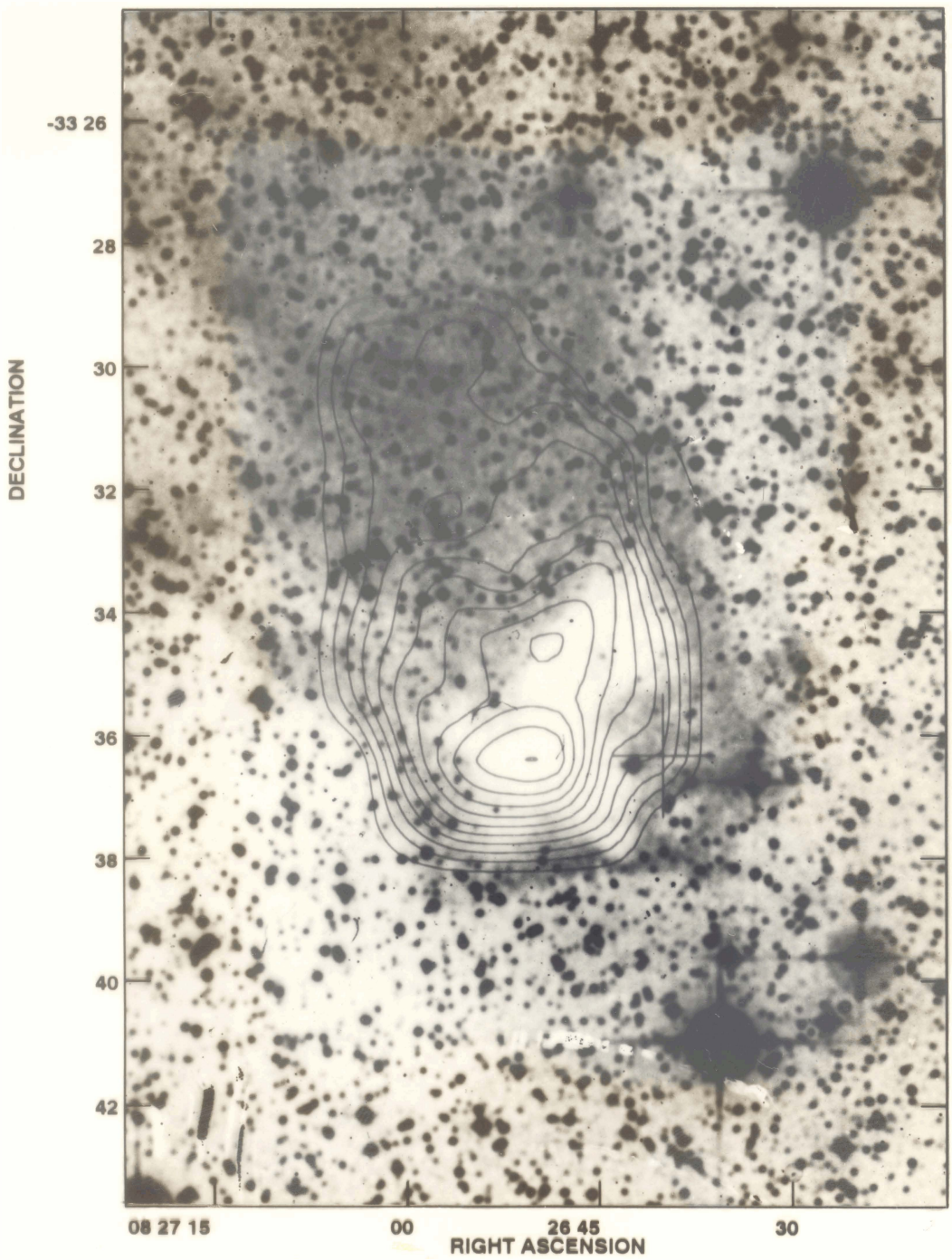

Figure 5.5: Contours of the ^{13}CO column density superposed on an optical negative image of CG 22-Blob *1*. The lowest contour is at $8 \times 10^{14} cm^{-2}$ and the step size is 8 x $10^{14} cm^{-2}$.

maps. The virial mass is too large compared to the mass derived from CO observations. This may imply that the cloud is disintegrating due to the effects of its environment.

REFERENCES

Bally, J., Langer, W.D., Stark, A.A., Wilson, R.W. 1987, Ap. J., 312, L45.

Dickman, R.L., 1978, *Ap.* J. Suppl., 37, 407.

Sahu, M., Pottasch, S.R., Sahu, K.C., Wesselius, P.R., Desai, J.N. 1988, Astron. Astrophys., 195, 269.

Sugitani, K., Fukui, Y., Mizuno, A. and Ohashi, N. 1989, Ap. *J.(Letters)*, 342, L87.

Frerking, M.A., Langer, W.D., Wilson, R.W. 1982, *Ap.* J., 262, 590.

Snell, R.L., Scoville, N.Z., Sanders, D.B., Erickson, N.R. 1984, Ap. J., 284, 176.

Solomon, P.M., Rivolo, A.R., Barret, J.W., Yahil, A. 1987, Ap. J., 319, 730.

Ulich, B.L., Haas, R.W. 1976, *Ap.* J. *Suppl.*, 30, 247.

Young, J.S., Scoville, N.Z. 1982 *Ap.* J., 258, 467.